

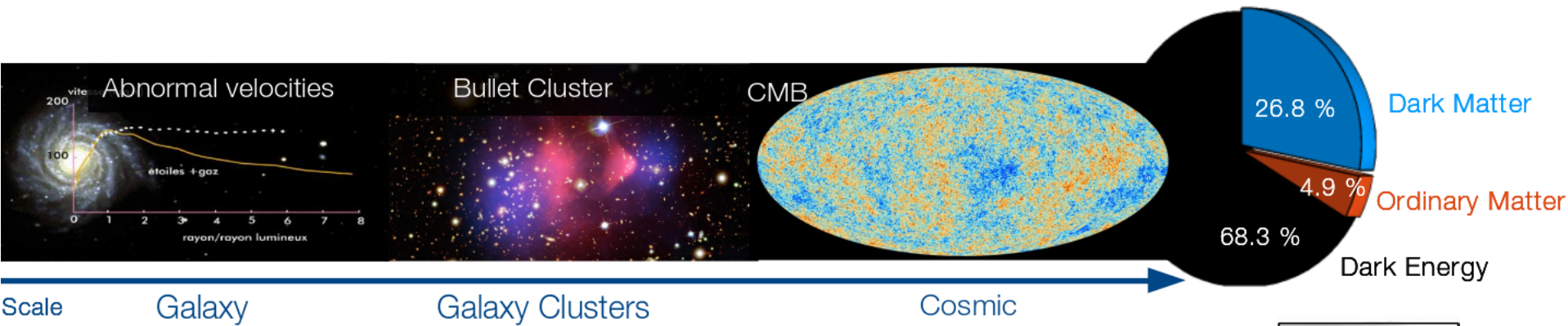
NEWS-G: Calibration data from the LSM

Daniel Durnford
Supervisor: Prof. Marie-Cécile Piro

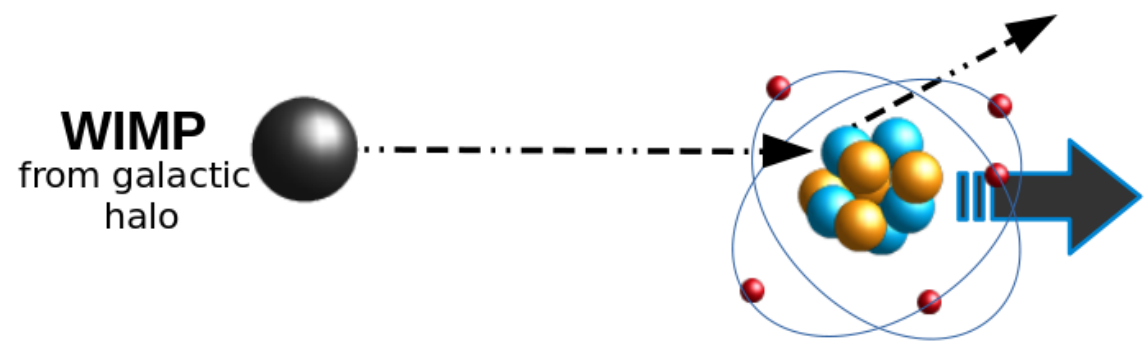
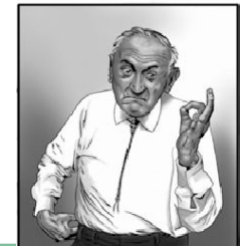
CAP Congress 2020
June 8th



Direct detection of dark matter



Evidence for the existence of dark matter has accumulated for almost 100 years! Particle dark matter is a leading hypothesis.



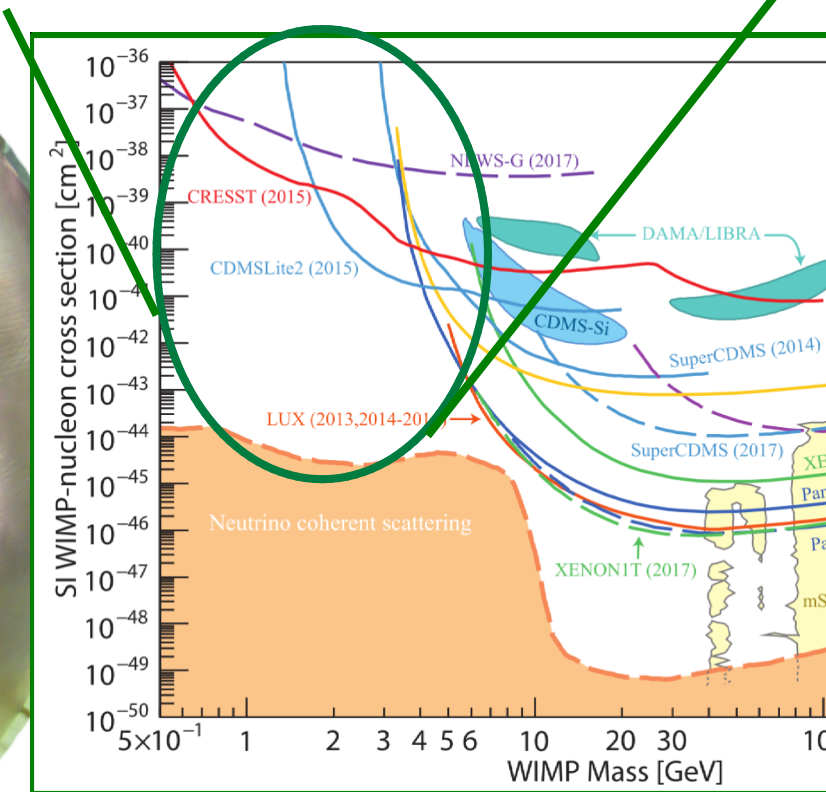
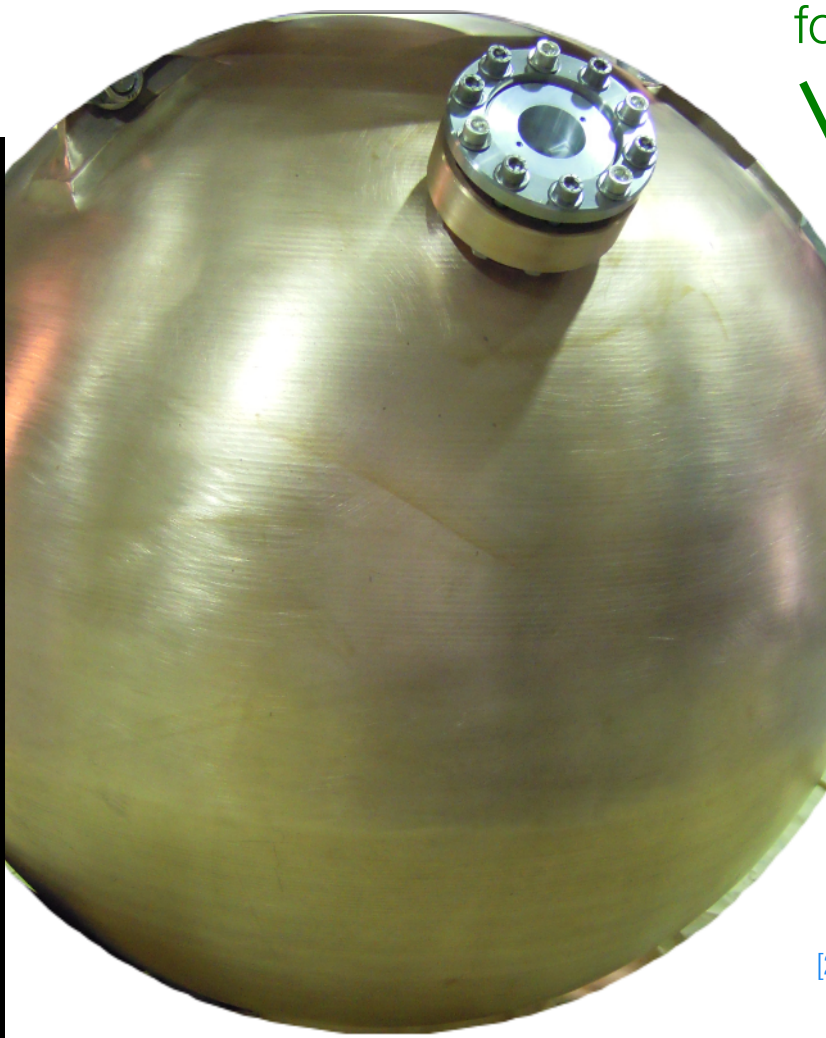
Minuscule energy depositions:
Recoils of $E_R \leq 1$ keV

Direct detection: searching for elastic scattering of (historically) WIMP dark matter off atomic nuclei

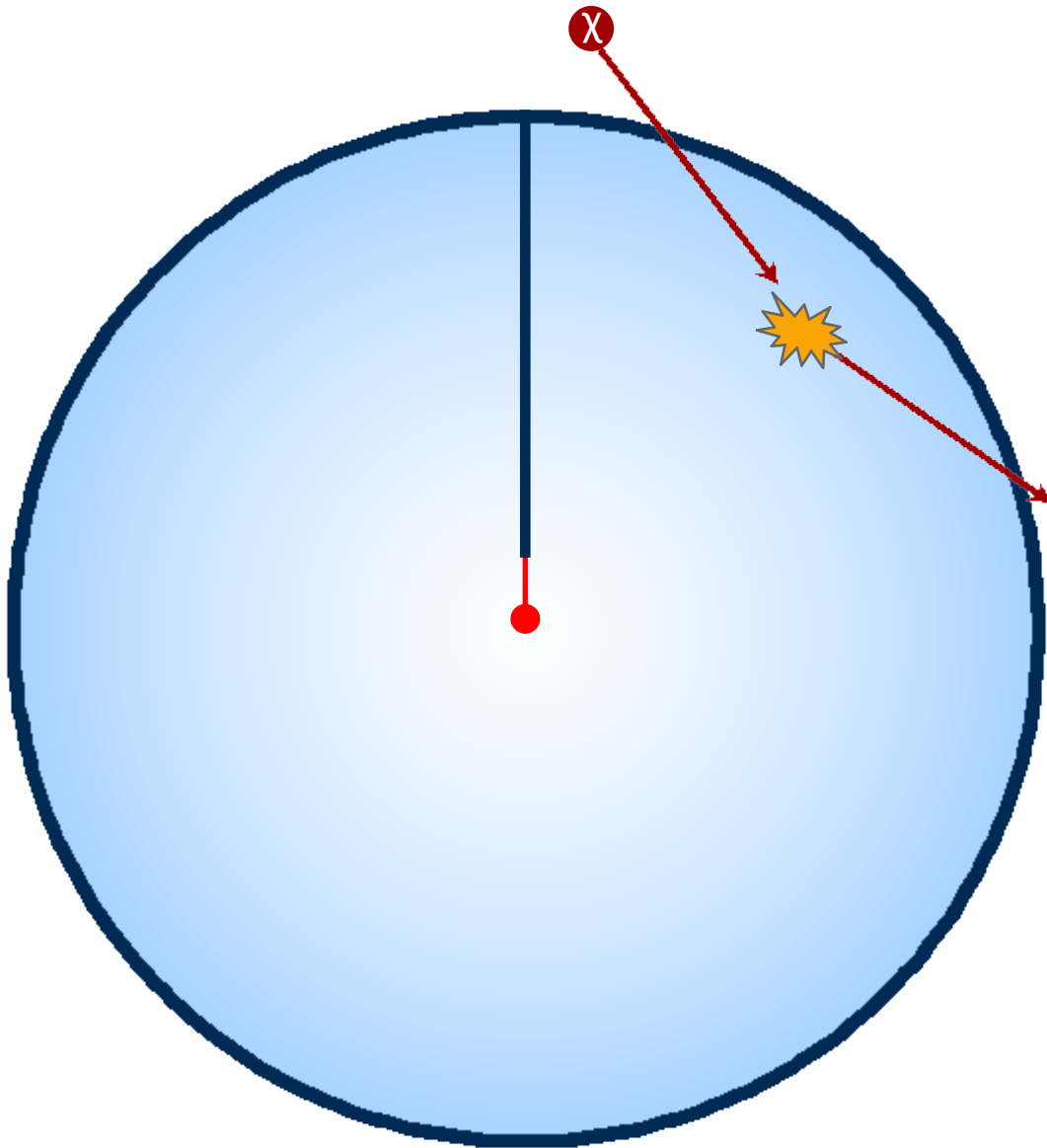
The NEWS-G dark matter experiment

Spherical Proportional Counters (SPCs) to search for low-mass dark matter

Absence of canonical WIMPs motivates searches for other low mass DM candidates



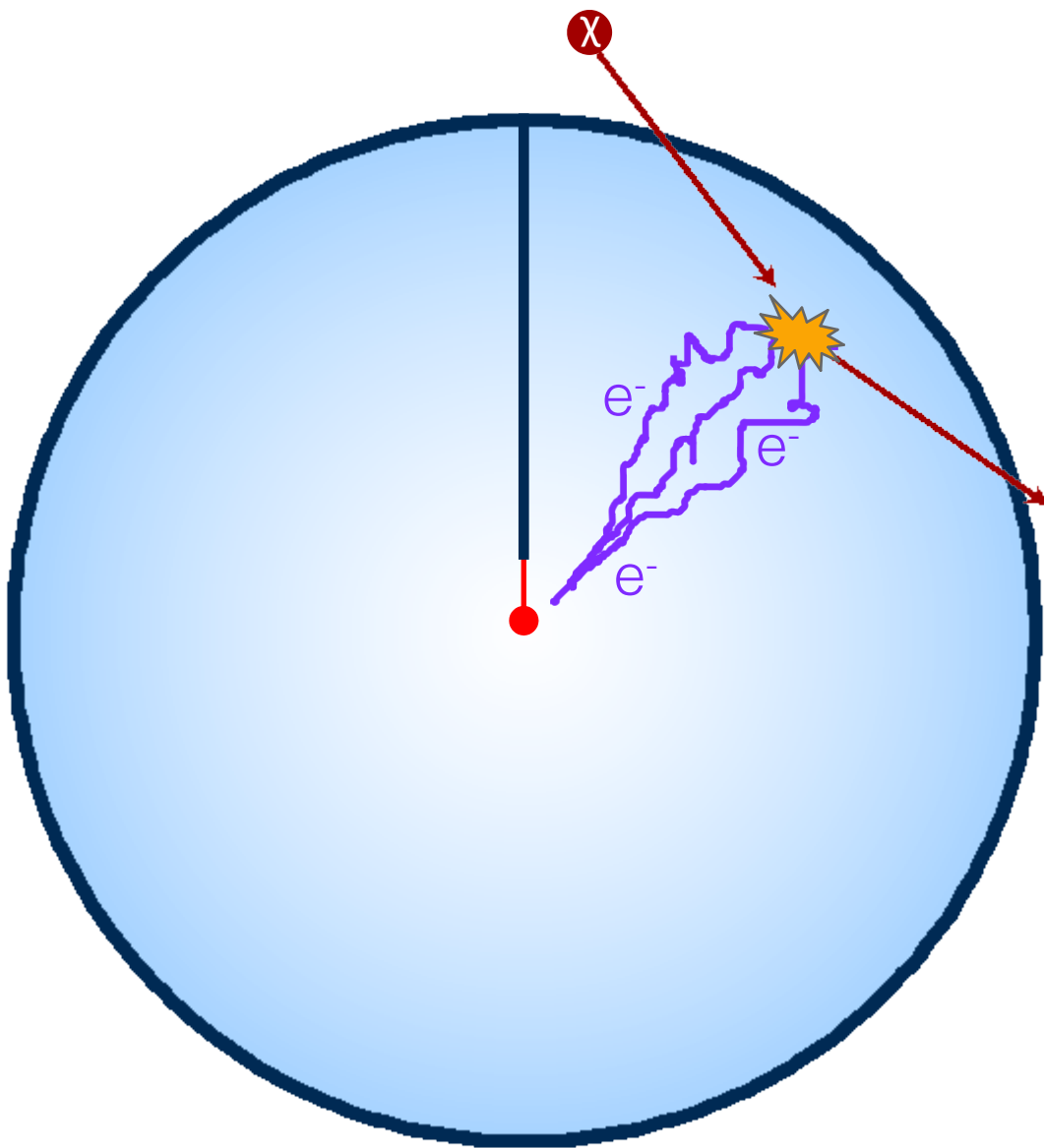
[1] D. Bauer et al, Phys. Dark Univ., 7–8, 16–23 (2015)
[2] K. Petraki et al, Int. J. Mod. Phys. A, 28(19), 1330028 (2013)
[4] K.M. Zurek, Phys. Rep., 537(3), 91 (2014)
[4] R. Essig et al, Dark Sectors and New, Light, Weakly-Coupled Particles (2013)



(1) Primary Ionization

$$\langle \#PE \rangle = \frac{E}{W(E)}$$

$$W_{nr} = W_{\gamma}/Q(E) \quad \text{Neon: } W_{\gamma} \sim 36 \text{ eV/pair} \\ Q \sim 0.2$$



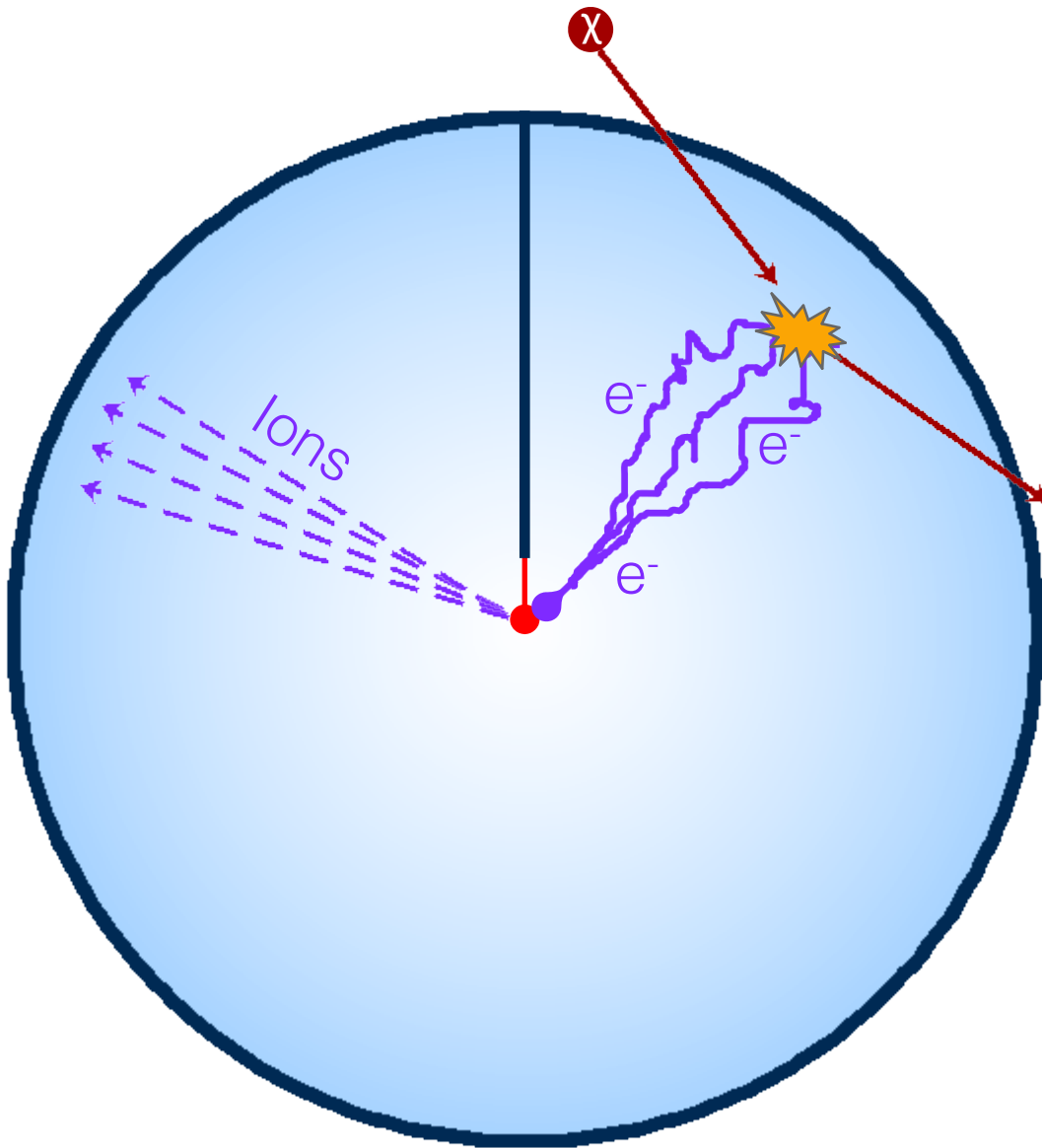
(1) Primary Ionization

$$\langle \#PE \rangle = \frac{E}{W(E)}$$

$$W_{nr} = W_{\gamma}/Q(E) \quad \text{Neon: } W_{\gamma} \sim 36 \text{ eV/pair} \\ Q \sim 0.2$$

(2) Drift of charges

Radially-dependent diffusion allows for fiducialization



(1) Primary Ionization

$$\langle \#PE \rangle = \frac{E}{W(E)}$$

$$W_{nr} = W_{\gamma}/Q(E) \quad \text{Neon: } W_{\gamma} \sim 36 \text{ eV/pair} \\ Q \sim 0.2$$

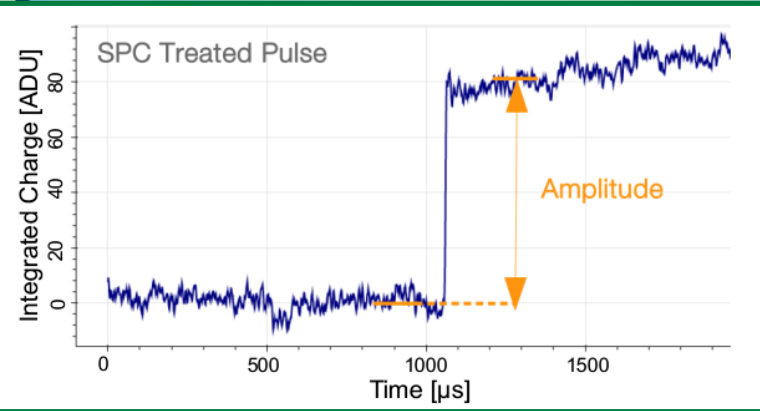
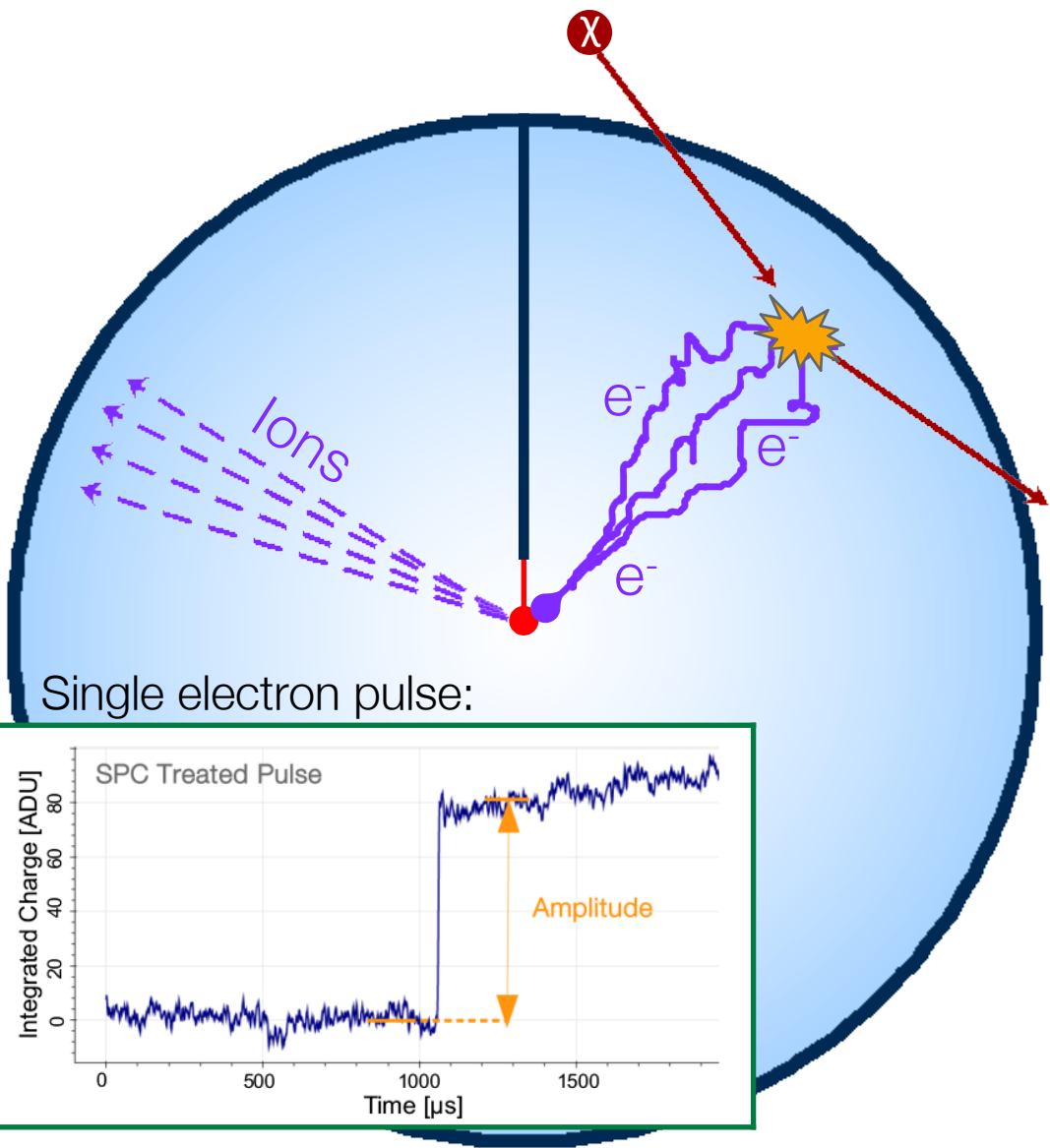
(2) Drift of charges

Radially-dependent diffusion allows for fiducialization

(3) Avalanche of secondary e⁻/ion pairs

Amplification of signal through Townsend avalanche (tunable with V)

Principle of operation



(1) Primary Ionization

$$\langle \#PE \rangle = \frac{E}{W(E)}$$

$$W_{nr} = W_{\gamma}/Q(E) \quad \text{Neon: } W_{\gamma} \sim 36 \text{ eV/pair} \\ Q \sim 0.2$$

(2) Drift of charges

Radially-dependent diffusion allows for fiducialization

(3) Avalanche of secondary e⁻/ion pairs

Amplification of signal through Townsend avalanche (tunable with V)

(4) Signal formation

Current induced by the secondary ions drifting away from anode

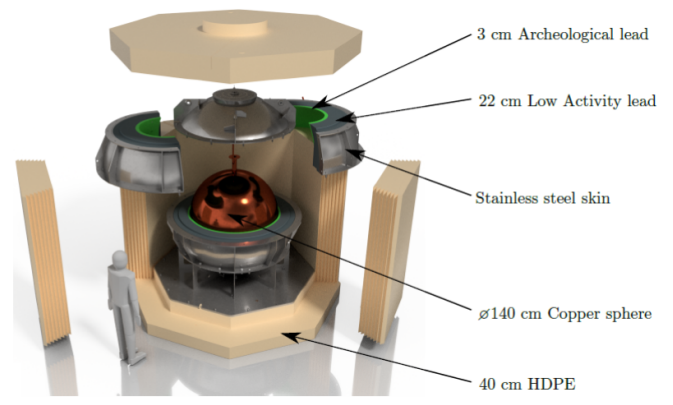
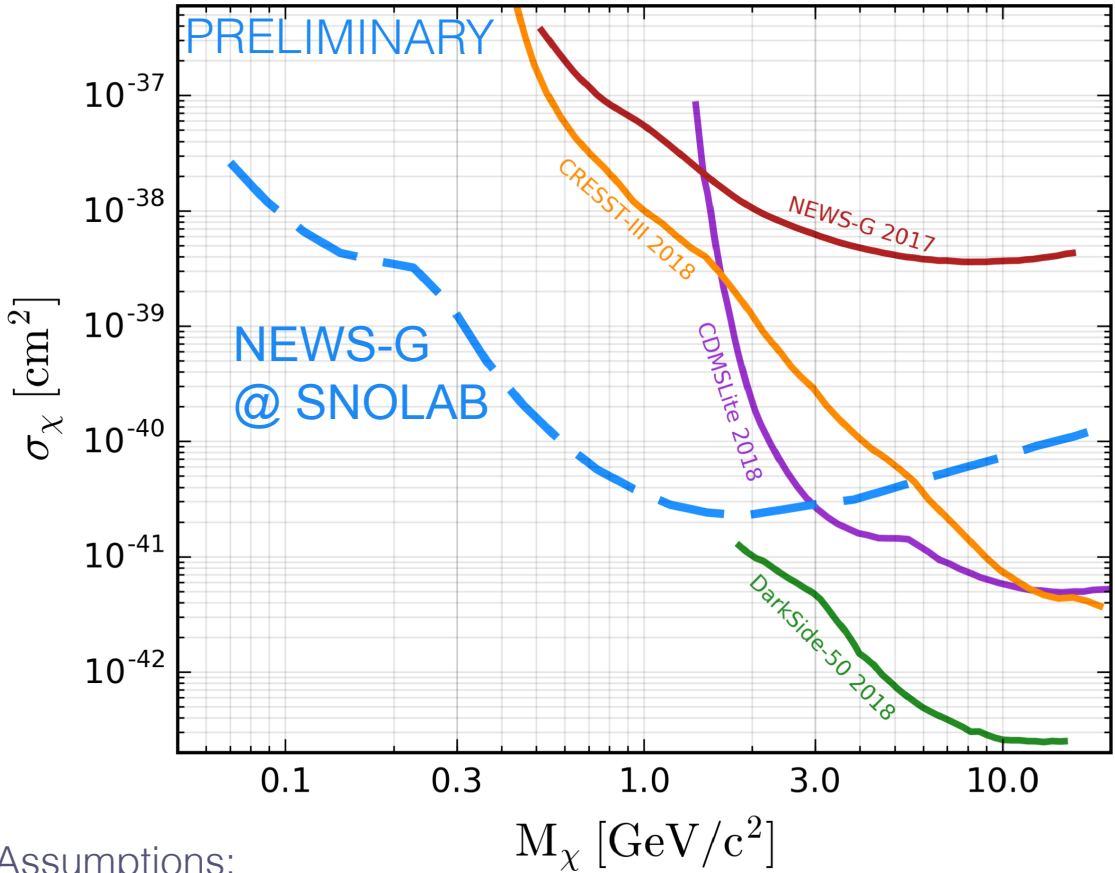
(5) Signal readout

Current integrated and digitized

Preparing for NEWS-G @ SNOLAB

NEWS-G is preparing to install a new detector at **SNOLAB** in winter 2020!

Expected to be sensitive to WIMP masses ~ 100 MeV using H-rich gas and an energy threshold < 50 eV_{nr}



Assumptions:
 Ne + 10% CH₄, Exposure: 20 kg days, F = 0.2, θ = 0.12,
 SRIM quenching factor, Background: 1.78 dru,
 ROI: 14 eV_{ee} - 1 keV_{ee}, Optimum Interval Method

Commissioning data was taken at the LSM:

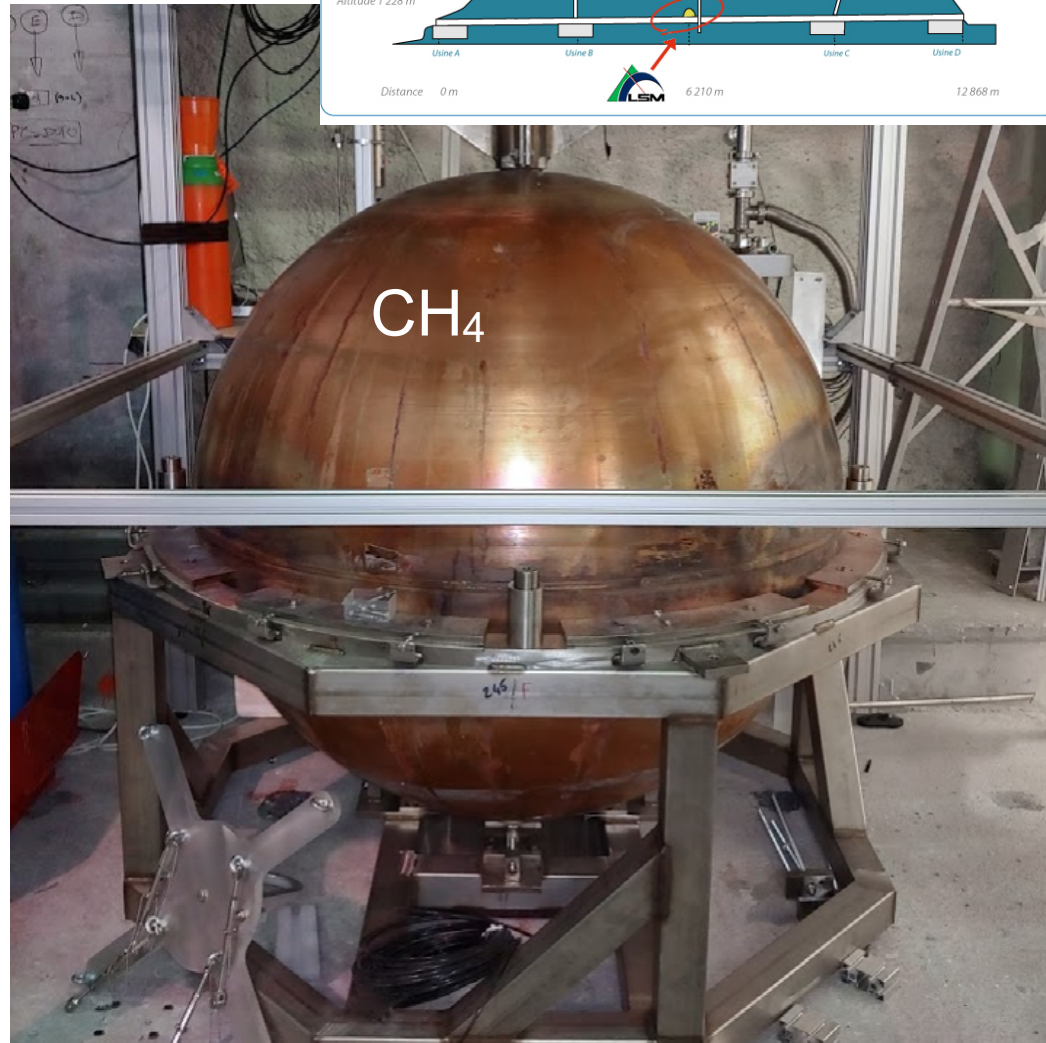
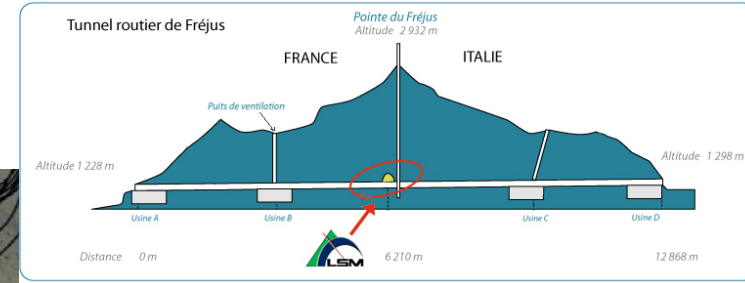


A water tank was used instead of the PE shield. First test of sensor deployment system, electronics

Data taken with

135 mbar of pure CH₄:

- » Larger fraction of hydrogen for low-mass DM sensitivity
- » More transparent to high energy γ 's, lower background rate / unit mass than Ne/CH₄ mixture

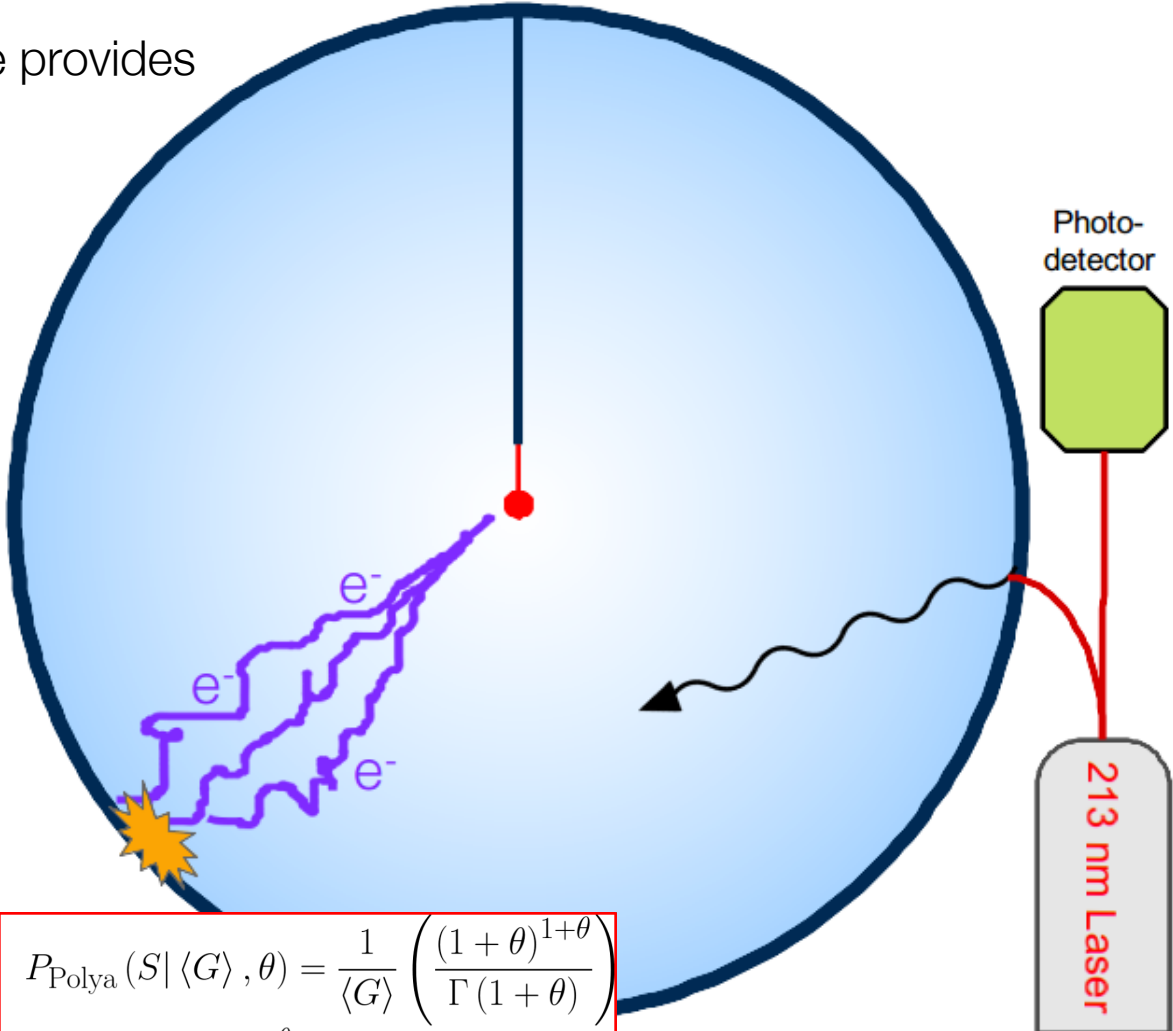
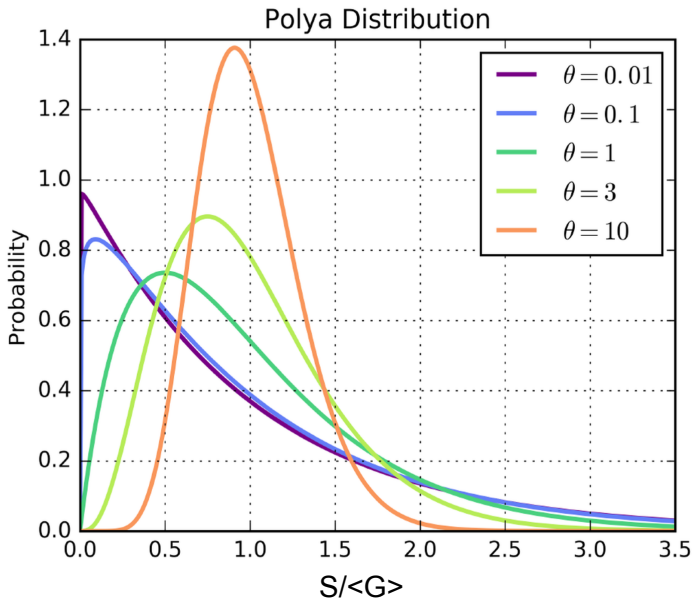


UV laser calibration

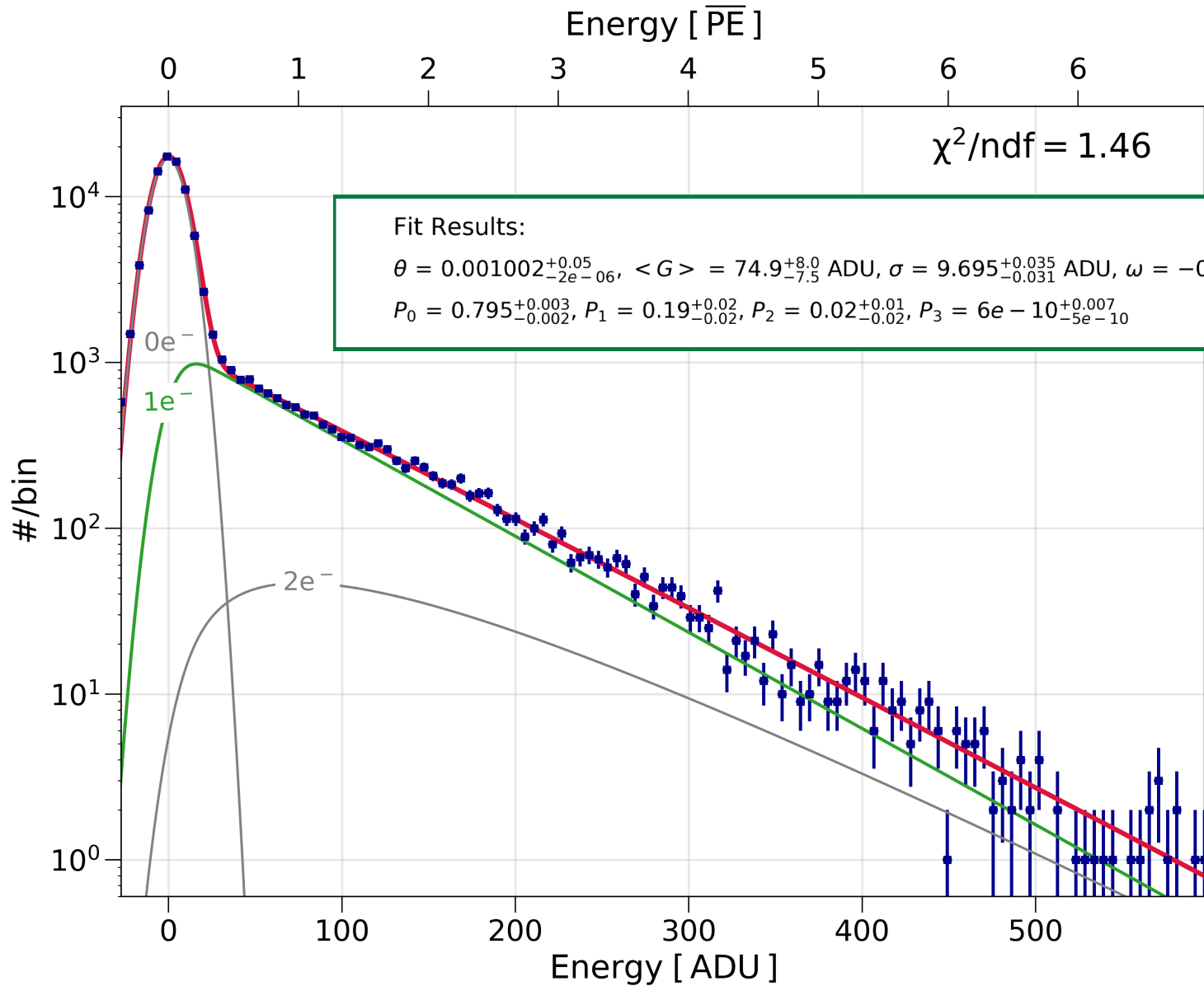
Q. Arnaud et al. (NEWS-G Collaboration), Phys. Rev. D 99, 102003 (2019)

UV laser with parallel photo-diode provides tagged source of single (or a few) primary electrons

Can confirm model of avalanche statistics (Polya distribution), provide estimates of empirical parameters:

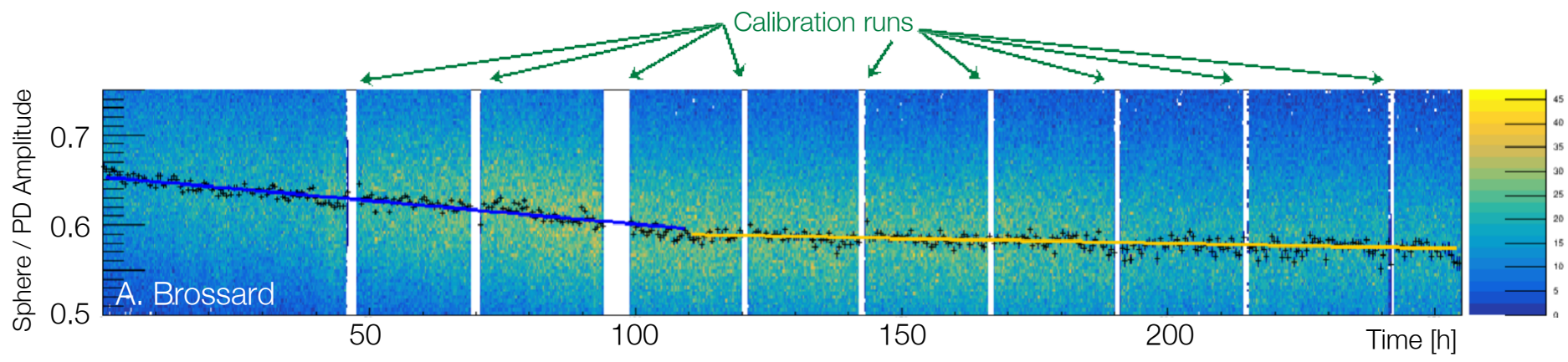


$$P_{\text{Polya}}(S | \langle G \rangle, \theta) = \frac{1}{\langle G \rangle} \left(\frac{(1 + \theta)^{1+\theta}}{\Gamma(1 + \theta)} \right) \times \left(\frac{S}{\langle G \rangle} \right)^\theta \exp \left(- (1 + \theta) \frac{S}{\langle G \rangle} \right)$$



Detector stability

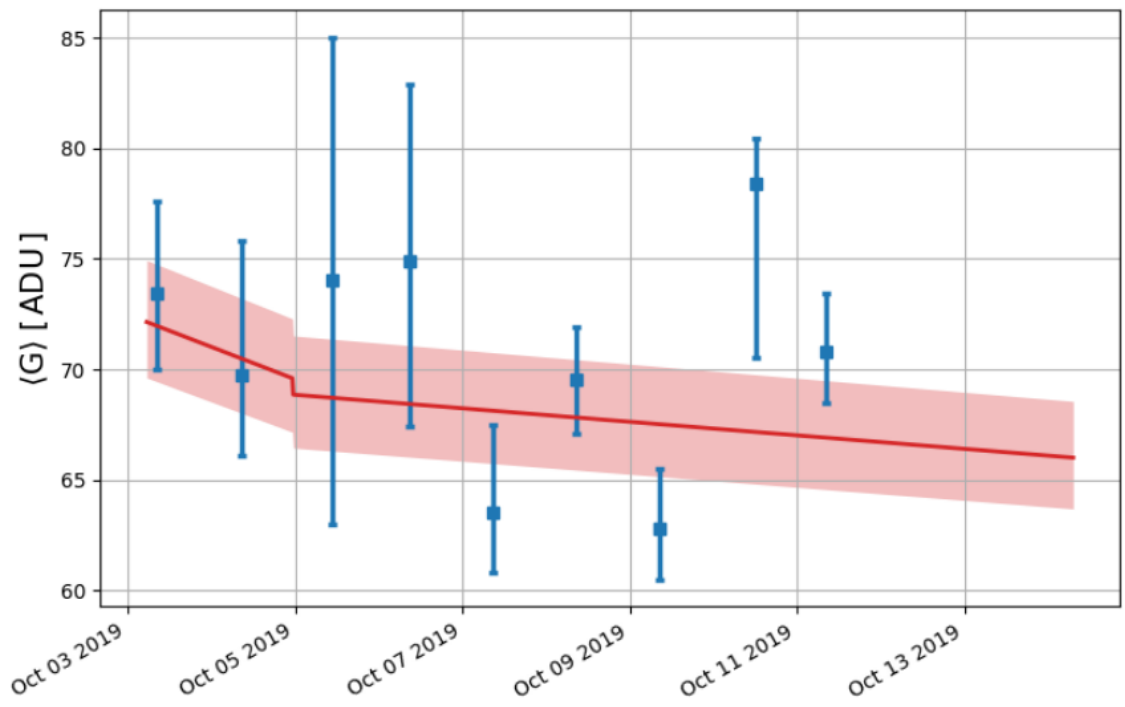
UV laser also used to monitor the detector response during physics data collection



Slow change in the detector gain over time due to gas quality degradation

In-run data can be used to determine the fractional change in gain over time

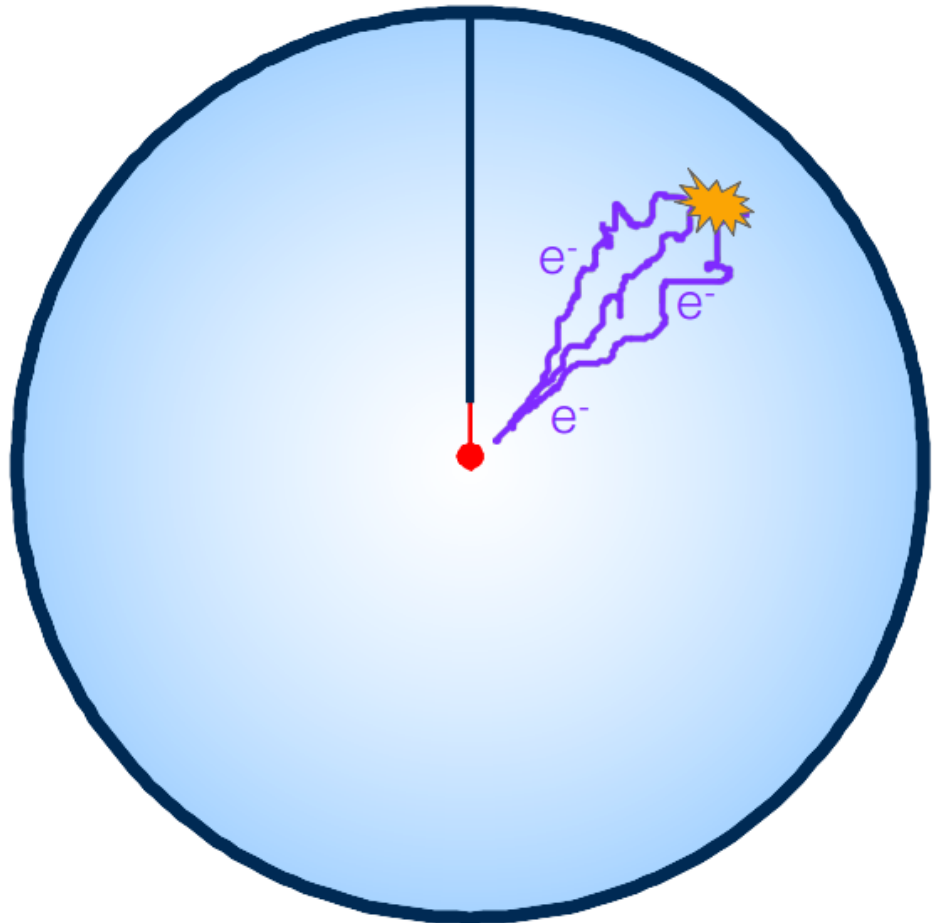
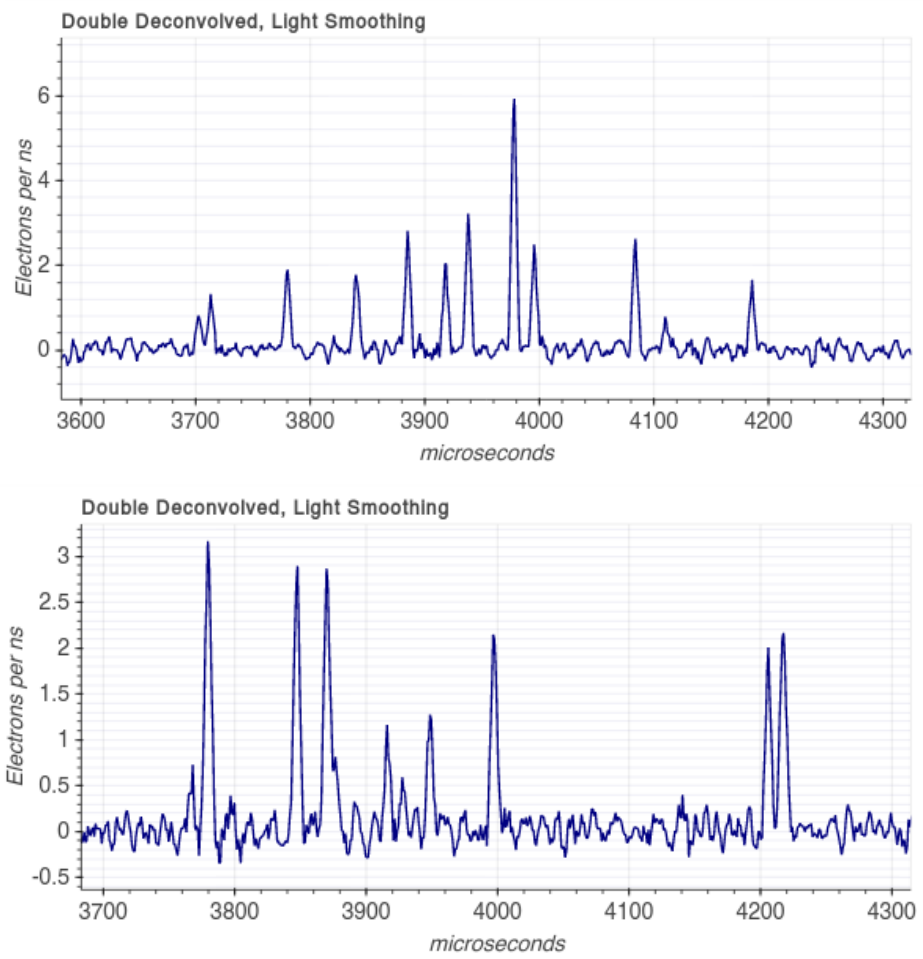
Daily dedicated laser calibrations can be used to determine absolute value of gain over time



Primary electron finding

The large drift volume allows us to resolve individual primary electrons in time!

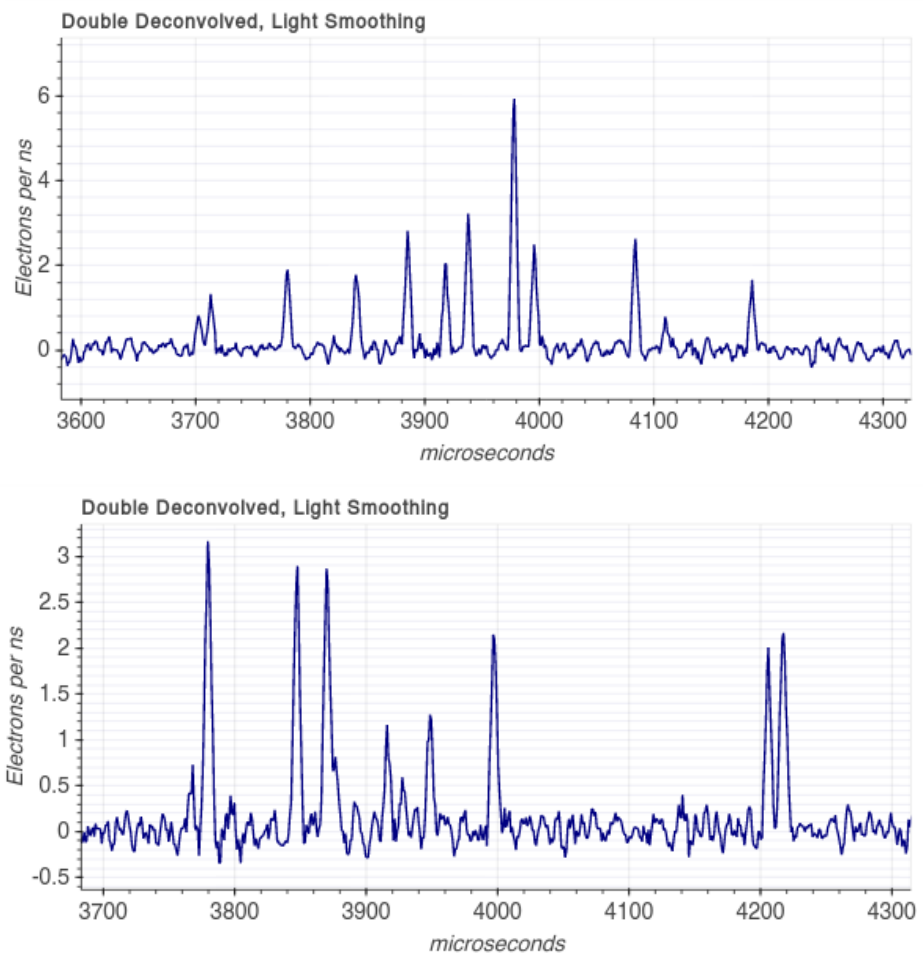
UV Laser events from new 140cm SPC:



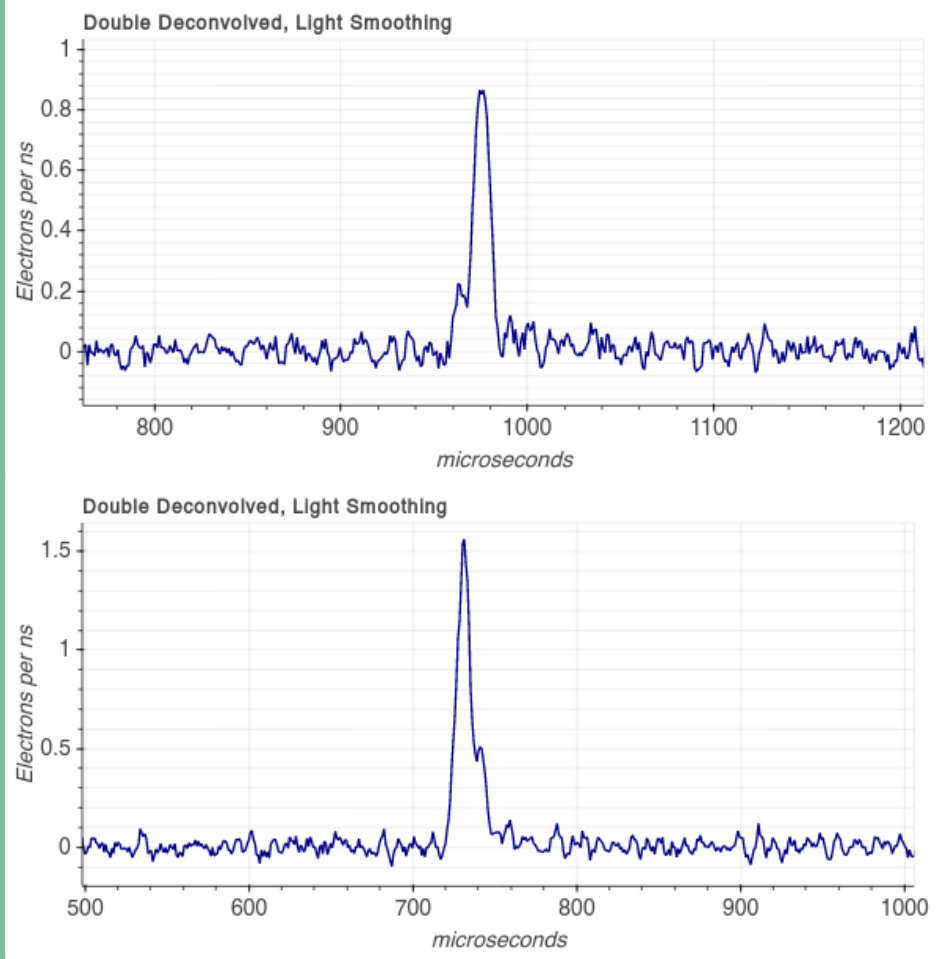
Primary electron finding

The large drift volume allows us to resolve individual primary electrons in time!

UV Laser events from new 140cm SPC:



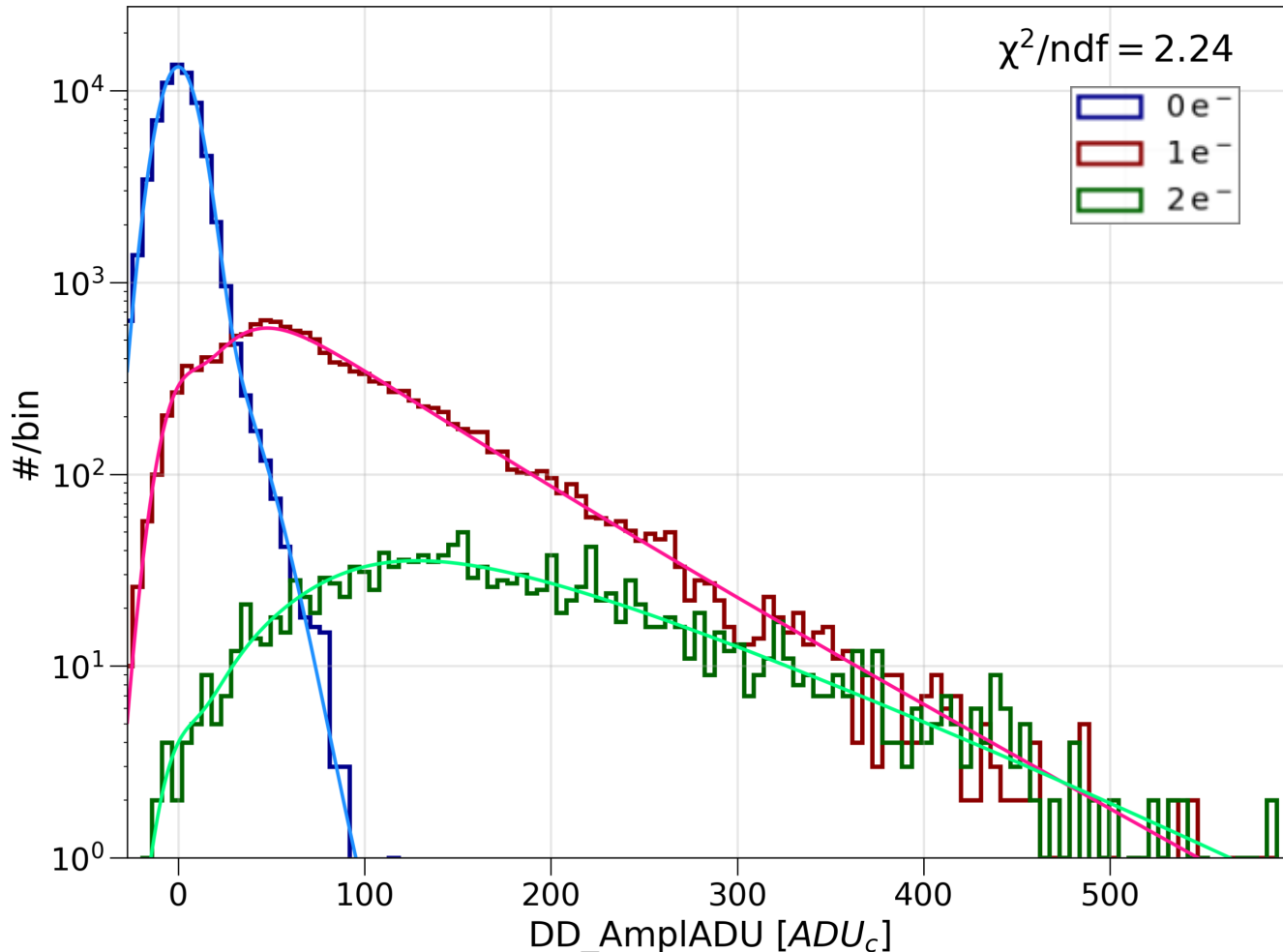
³⁷Ar events from 30cm prototype SPC:





Primary electron finding

To characterize the performance of this peak-finding, we can fit the laser data resolved into its component spectra. There are contributions from:



- » False negatives: true electron below peak-finding threshold
- » False positive: misidentification of noise
- » Coincidences: multiple true electrons grouped together

Good agreement between methods for relevant parameters

Combined spectra:

$$\theta = 0.011^{+0.004}_{-0.004}, \langle G \rangle = 72.11^{+0.99}_{-0.97} \text{ ADU}$$

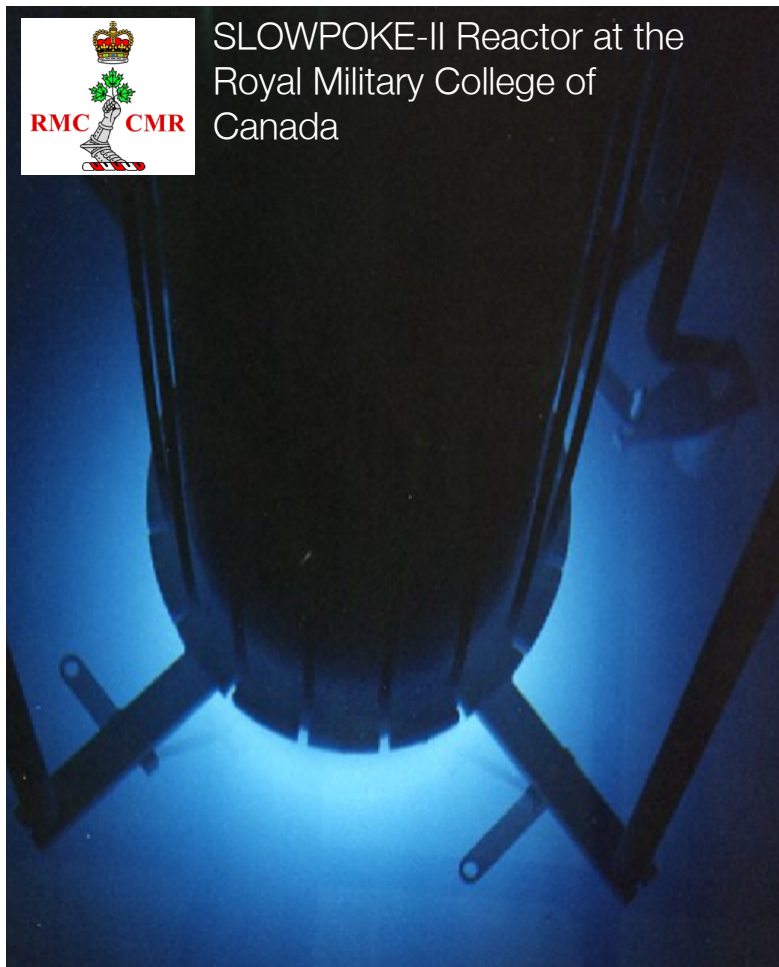
Resolved Spectra:

$$\theta = 0.0012^{+0.02}_{-0.0002}, \langle G \rangle = 69.7^{+6.1}_{-3.6} \text{ ADU}$$

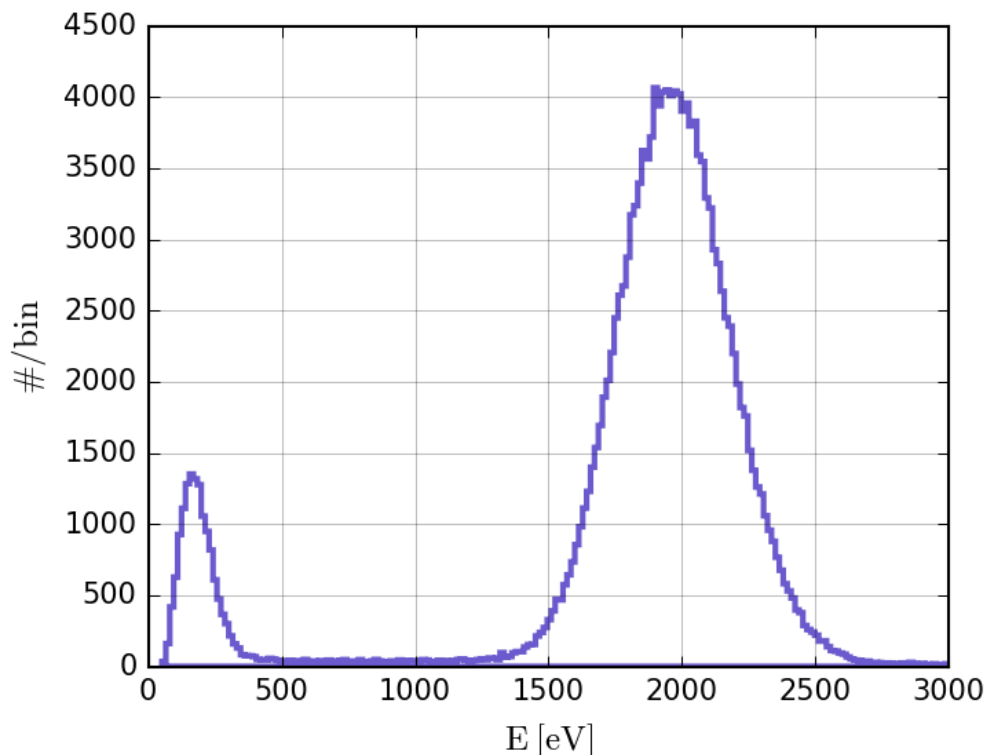
^{37}Ar measurements

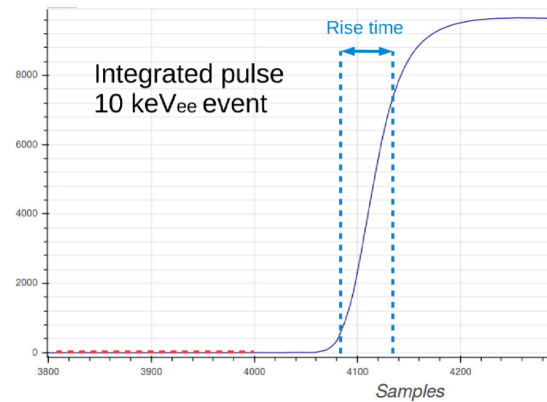
^{37}Ar : radioactive gas that decays via electron capture. But with a 35 day half life, we need a way to produce samples at regularly:

D.G. Kelly et al., *Journal of Radioanalytical and Nuclear Chemistry* 318(1) (2018).



Decay produces 2.82 keV and 270 eV x-rays, generated uniformly throughout the detector:



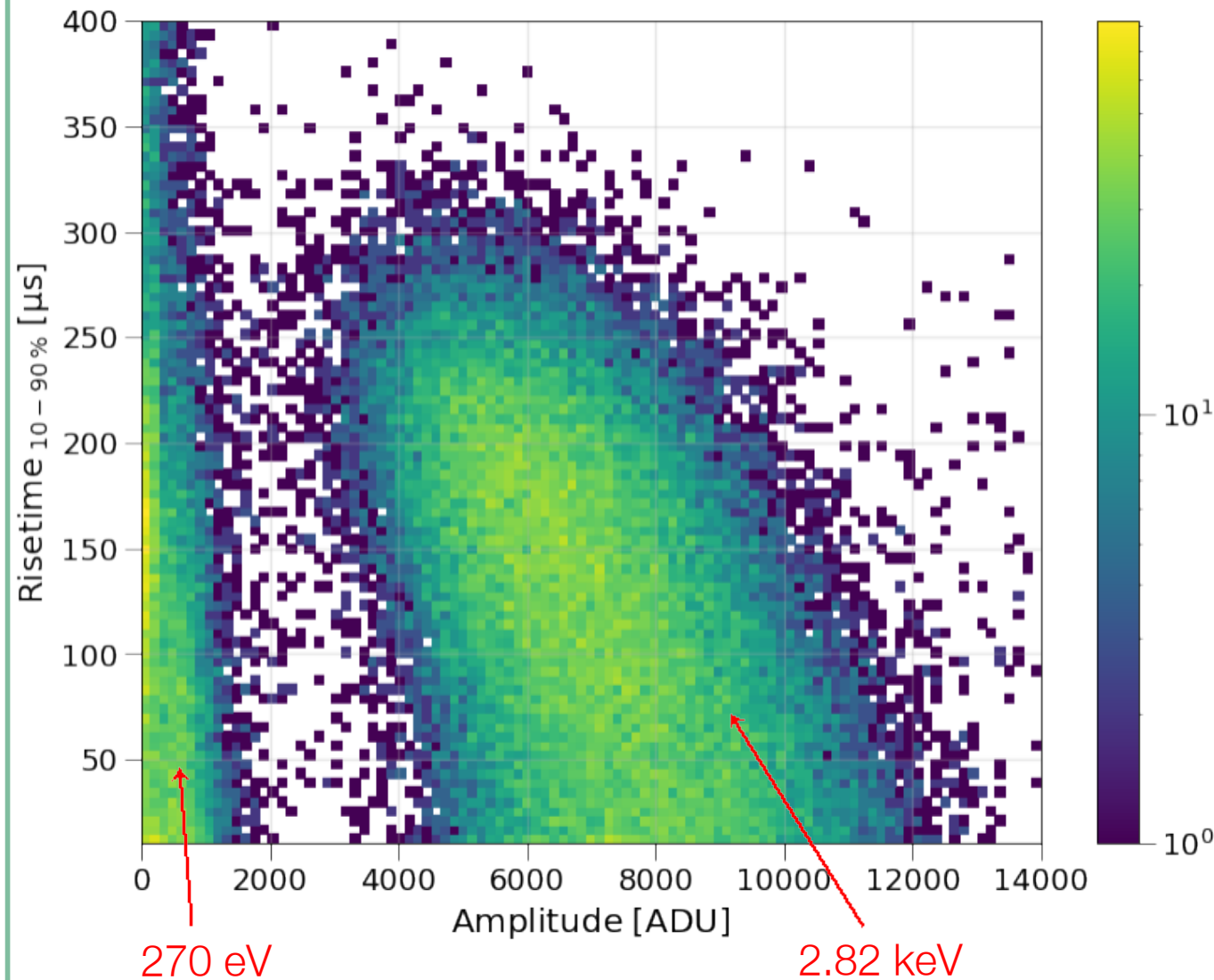


Risetime is a PSD variable that is the “slope” of the leading edge of a pulse

Larger for surface events due to greater diffusion of primary electrons

-> Risetime is correlated with radial position

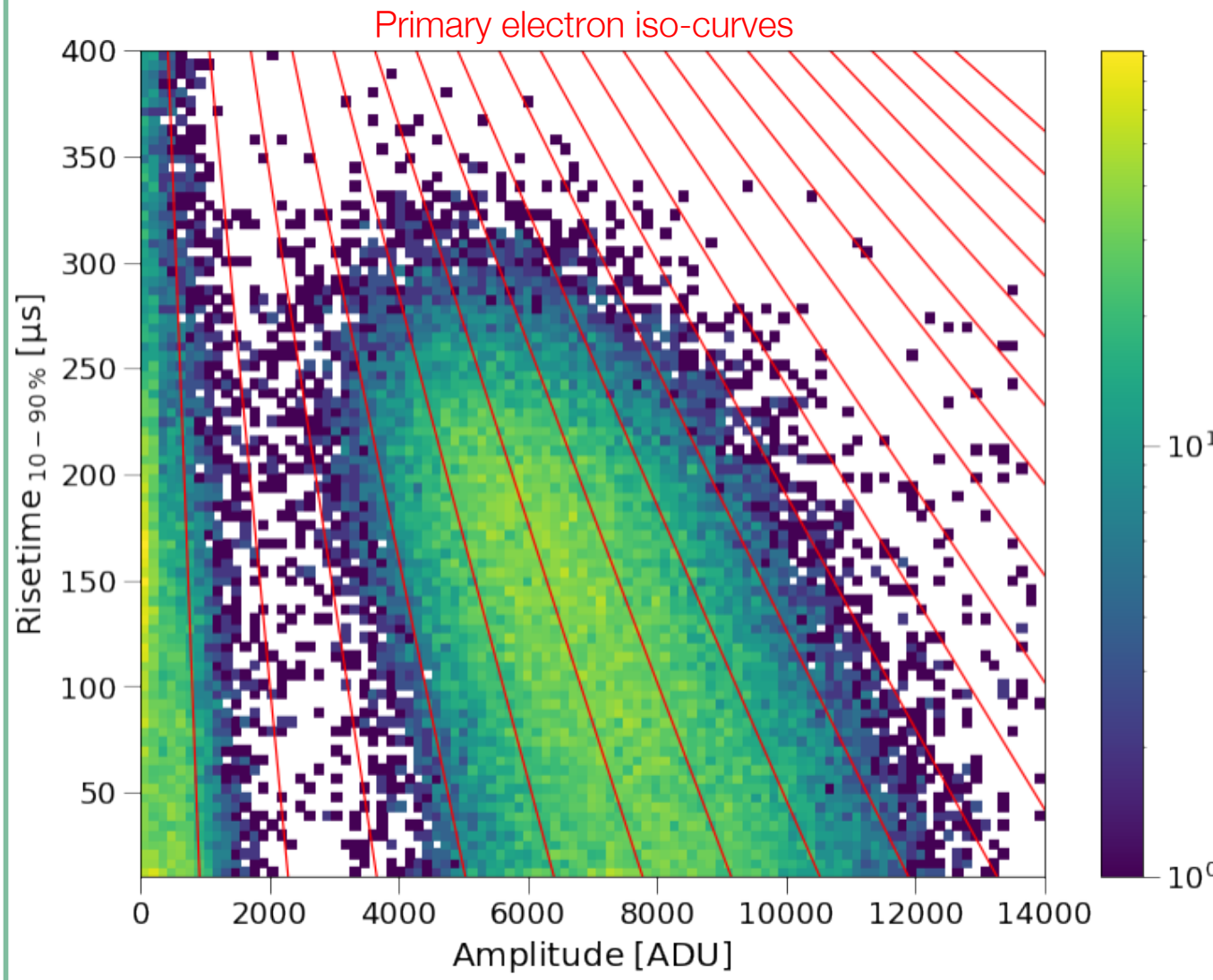
Ar-37 calibration data:



Charge trapping

Charge trapping of primary electrons with oxygen contamination leads to reduced amplitudes at higher risetimes (events far from the anode)

This can be modelled with binomial statistics for the surviving # of primary electrons, and a survival probability that is a linear function of risetime



Modelling primary ionization

The “Fano factor” is an empirical parameter describing dispersion in primary ionization

$$F = \frac{\sigma^2}{\mu}$$

Known to be ~ 0.2 for noble gases:

Medium	F
Si	0.155 ± 0.002 (3 keV e ⁻)
	0.134 ± 0.003 (F-Kα)
Ar	0.23 ± 0.05 (⁵⁵ Fe)
	0.20 ± 0.02 (5.3 MeV α)
Ar+0.8% CH4	0.19 (5.68 MeV α)
Xe (gas)	0.170 ± 0.007 (soft x-rays)
Ge	0.121 ± 0.001 (Al-Kα)

No probability distribution is a priori known to represent ionization statistics. Sparse and inconsistent measurements demands a flexible modelling tool

Modelling primary ionization

The “Fano factor” is an empirical parameter describing dispersion in primary ionization

$$F = \frac{\sigma^2}{\mu}$$

Known to be ~ 0.2 for noble gases:

Medium	F
Si	0.155 ± 0.002 (3 keV e ⁻)
	0.134 ± 0.003 (F-Kα)
Ar	0.23 ± 0.05 (⁵⁵ Fe)
	0.20 ± 0.02 (5.3 MeV α)
Ar+0.8% CH4	0.19 (5.68 MeV α)
Xe (gas)	0.170 ± 0.007 (soft x-rays)
Ge	0.121 ± 0.001 (Al-Kα)

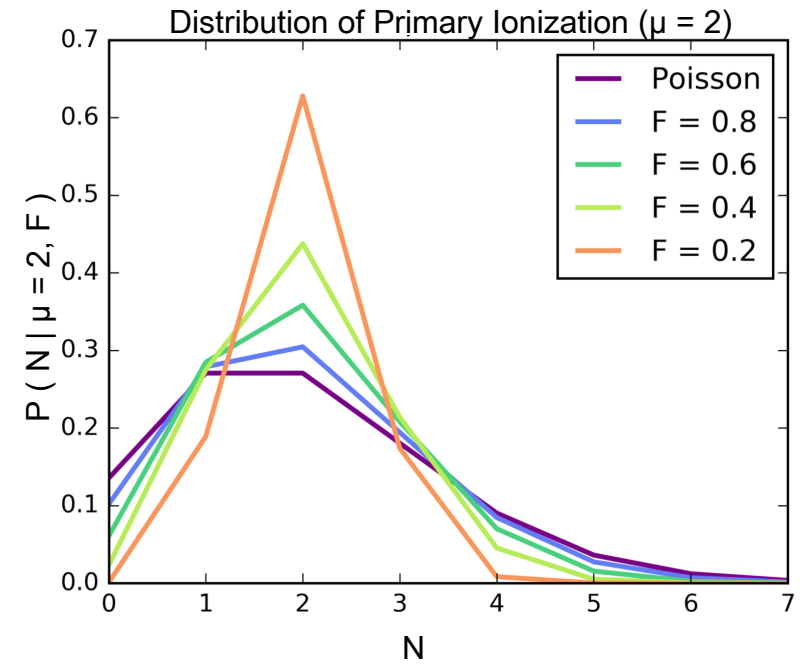
No probability distribution is a priori known to represent ionization statistics. Sparse and inconsistent measurements demands a flexible modelling tool

We use the COM-Poisson distribution:

$$P(x|\lambda, \nu) = \frac{\lambda^x}{(x!)^\nu Z(\lambda, \nu)}$$

$$Z(\lambda, \nu) = \sum_{j=0}^{\infty} \frac{\lambda^j}{(j!)^\nu} \quad \lambda \in \{\mathbb{R} > 0\}, \quad \nu \in \{\mathbb{R} \geq 0\}$$

D. Durnford, Q. Arnaud, and G. Gerbier Phys. Rev. D 98, 103013 (2018)



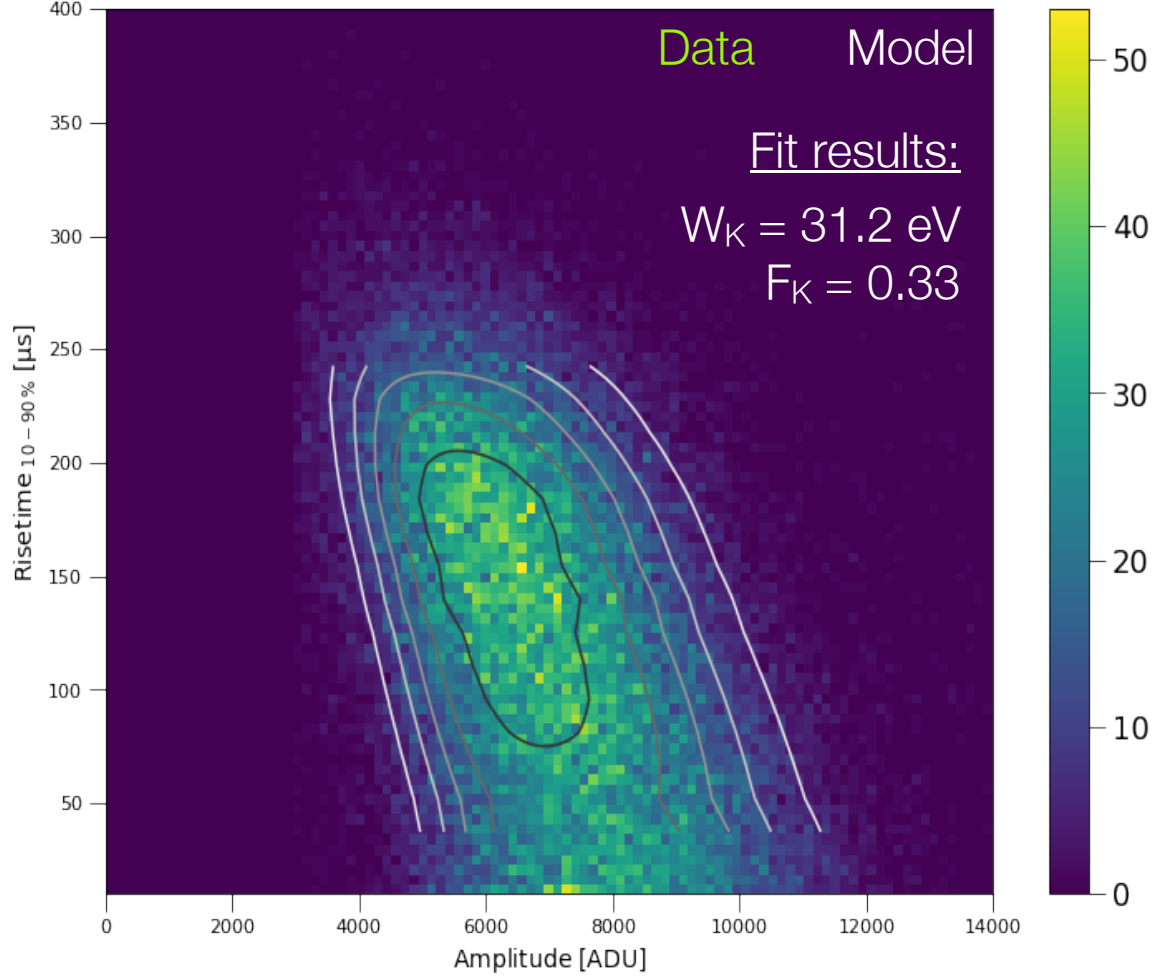
CH₄ data results

The analysis of ~12 days of data with 135 mbar pure CH₄ at the LSM is ongoing

Calibration from a UV laser and ³⁷Ar are the primary tools for understanding the detector response at the level of single ionizations

Results expected within the year, which will be the **first DM limit set with hydrogen target atoms!**

Preliminary fit results:

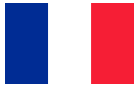


Thank you!



Queen's University Kingston - G Gerbier, G Giroux, R Martin, S Crawford, M Vidal, G Savvidis, A Brossard, F Vazquez de Sola, K Dering, V Millious, J McDonald, M Van Ness, M Chapellier, P Gros, JM Coquillat, JF Caron, L Balogh

- Copper vessel and gas set-up specifications, calibration, project management
- Gas characterization, laser calibration on smaller scale prototypes
- Simulations/Data analysis



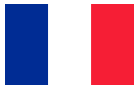
IRFU (Institut de Recherches sur les Lois fondamentales de l'Univers)/**CEA Saclay - I Giomataris**, M Gros, JP Mols

- Sensor/rod (low activity, optimization with 2 electrodes)
- Electronics (low noise preamps, digitization, stream mode)
- DAQ/soft



Aristotle University of Thessaloníki - I Savvidis, A Leisos, S Tzamarias

- Simulations, neutron calibration
- Studies on sensor



LPSC/LSM Laboratoire de Physique Subatomique et Cosmologie, Laboratoire Souterrain de Modane) **Grenoble - D Santos**, M Zampaolo, A DastgheibiFard JF Muraz, O Guillaudin

- Quenching factor measurements at low energy with ion beams
- Low activity archaeological lead
- Coordination for lead/PE shielding and copper sphere



Pacific Northwest National Laboratory - E Hoppe, R Bunker

- Low activity measurements, copper electro-forming

The NEWS-G Collaboration
(June 2020)



RMCC Kingston - D Kelly, E Corcoran, L Kwon

- ^{37}Ar source production, sample analysis



SNOLAB Sudbury - P Gorel, S Langrock

- Calibration system/slow control



University of Birmingham - K Nikolopoulos, P Knights, I Katsioulas, R Ward

- Simulations, analysis, R&D



University of Alberta - MC Piro, D Durnford, Y Deng, P O'Brien

- Gas purification, data analysis



Associated labs: TRIUMF - F Retiere

